



# Three-dimensional simulation of CVD diamond film growth

S. Barrat, P. Pigeat, E. Bauer-Grosse

## ► To cite this version:

S. Barrat, P. Pigeat, E. Bauer-Grosse. Three-dimensional simulation of CVD diamond film growth. *Diamond and Related Materials*, 1996, 5 (3-5), pp.276-280. 10.1016/0925-9635(95)00424-6 . hal-03978970

**HAL Id: hal-03978970**

**<https://hal.univ-lorraine.fr/hal-03978970>**

Submitted on 10 Feb 2023

**HAL** is a multi-disciplinary open access archive for the deposit and dissemination of scientific research documents, whether they are published or not. The documents may come from teaching and research institutions in France or abroad, or from public or private research centers.

L'archive ouverte pluridisciplinaire **HAL**, est destinée au dépôt et à la diffusion de documents scientifiques de niveau recherche, publiés ou non, émanant des établissements d'enseignement et de recherche français ou étrangers, des laboratoires publics ou privés.



Distributed under a Creative Commons Attribution - NonCommercial - NoDerivatives 4.0 International License

# THREE-DIMENSIONAL SIMULATION OF CVD DIAMOND FILM GROWTH

**S. Barrat, P. Pigeat, E. Bauer-Grosse**

Laboratoire de Science et Génie des Surfaces

Ecole des Mines, Parc de Saurupt 54042 NANCY Cedex (FRANCE)

## Abstract

As often reported in the case of CVD diamond synthesis, the elaboration conditions strongly affect the quality of the deposit in terms of roughness, grain boundary quantity, structural defect density or non diamond phase insertion. It is recognised that this quality mainly depends of the texture evolution. In our knowledge, it does not exist numerical simulations of this growth model that allow the diamond film quality to be predicted. In this way, we have developed a three-dimensional computer simulation of diamond growth. This numerical model is based on the homothetic growth of single diamond crystals in an Euclidean space and the selection of the enveloping surface obtained after the crystal interpenetration. By this way and in the limit of the exposed hypotheses, it is possible to build the topographies and to simulate its theoretical evolution's in the case of textured films synthesised on scratched silicon wafers according to the growth conditions such as the nucleation density, the growth rate ratio  $\alpha = \sqrt{3}(\frac{V_{100}}{V_{111}})$  or the synthesis time. We have particularly studied the ratio  $R_{\{hkl\}} = \left( \frac{S_{\{100\}}}{S_{\{100\}} + S_{\{111\}}} \right)$  of the topography according to the synthesis time, in order to follow the evolution of surface morphology.

## Introduction

Since late years now, the synthesis of diamond films by different chemical vapour deposition techniques (CVD techniques), and their mechanical, chemical and structural characterisations have shown that it was possible to obtain polycrystalline deposits on single crystal silicon substrates. These coatings with various thickness (ranging from nanometers to millimeters) are mainly polycrystalline (textured or heteroepitaxed), and can have physico-chemical properties approaching those of massive diamond. Nevertheless, the growth mode by islands of diamond on non-diamond

substrates induces the formation of chemical defects (presence of impurities or non-diamond carbon such as amorphous carbon or graphite) and structural defects (dislocations, twins, stacking faults and grain boundaries) that strongly affect the global quality of the film and consequently decrease the potentiality of applications generally admitted for this material.

A new way in the control of CVD diamond film elaboration consists to theoretically study the different steps of growth by using the evolutionary selection model, initially established by Van-der-Drift [1]. Its principles are remind hereafter. This model has been often used for the qualitative description of progressive fibre axis formation, when the shape of isolated crystals before the coalescence are known [2-7]. A more quantitative approach, reported in some works [8-10], is based of bidimensional numerical simulation that provides an evolutionary selection of square crystals by using of Van der Drift hypotheses. For initial conditions (density, morphology and orientation of the nuclei, growth rate), these simulations allow the prediction of the texture  $\langle hkl \rangle$  and the surface topography  $\{h_1k_1l_1\}\{h_2k_2l_2\}$ . This last terminology has been defined by Clausing et al.[3] to account for both the film texture  $\langle hkl \rangle$  and the type of facets located on the top of the film which are listed in order of abundance. These results are qualitatively in agreement with the experimental results, but are inevitably incomplete. Indeed, as reported by several authors [11-13], these bidimensional simulations don't take into account the steric effects associated to a three-dimensional growth where the crystal evolution depends on the all neighbouring crystals.

In this paper, we propose a simulation of the three-dimensional growth that produces a topography of the film surface. In the first section, we expose the indispensable hypotheses for the establishment of the calculus mode of this simulation in relation to the Van der Drift model. In the second section, we describe the main calculus steps and we present some topographies obtained for a low nucleation density. In the third section, we give the first results concerning the evolution of the ratio  $R_{\{hkl\}} = \left( \frac{S_{\{100\}}}{S_{\{100\}} + S_{\{111\}}} \right)$  as a function of the film thickness. In conclusion, we discuss the possible applications of this simulation in the field of materials and in the CVD process control.

### **The hypotheses of the three-dimensional model**

Our calculus is based on the fundamental hypotheses of the Van der Drift model. It supposes that the film growth occurs without secondary nucleation and the crystal morphology does not depend on their orientation. Consequently, the proposed numerical simulation is based on the homothetic growth in an Euclidean space of single diamond crystals (absence of multiply-twinned-Particles)

that are distributed in an aleatory manner over an unit surface (in our case  $100 \times 100 \mu\text{m}^2$ ) and which are only limited by smooth crystalline facets. The crystal morphology only depends on the growth parameter  $\alpha = \sqrt{3}(\frac{V_{100}}{V_{111}})$  initially defined by Wild et al.[9], and their apices are characterised by a family of triplets (x,y,z). The film formation consists to let the crystals independently grow without steric constraints, and for a given thickness, to recuperate the family of triplets (x,y,z) that constitute the enveloping surface. This hypothesis amounts to admit the volume interpenetration between neighbouring crystals. As reported by Thijssen et al.[12,13], this one does not exactly correspond to the evolutionary selection rule since the steric constraints must involve, and isolated emergence of a crystal through another one cannot occur (virtual emergence). Nevertheless, as illustrated fig.1, we can consider that these emergences do not strongly affect the topography for a sufficient thickness (or for a sufficient nucleation density). This figure shows the bidimensional growth concerning five crystals whose orientations are specially chosen to favour the pessimist case of the virtual emergence creation. With regard to the Van der Drift model, the crystals 1,2 and 3 have the same orientation (direction of fastest growth, denoted  $\vec{d}_{v\max}$ , normal to the substrate) in order to constitute the survival crystals for important thickness (fig.1E). The orientation of crystals 4 and 5 has been chosen in order to provoke the formation of virtual emergences when their interpenetrations with the crystals 1,2 and 3 occur. Figures 1A-C simulate the homothetic bidimensional growth of these five crystals without steric constraints. Fig.1D indicates the presence of several virtual emergences that are schematised by shaded areas. We can note that it is not possible to create a virtual emergence with a crystal whose  $\vec{d}_{v\max}$  is normal to the substrate (a virtual emergence is always provoked by a crystal having a weak angle between  $\vec{d}_{v\max}$  and the substrate). Taking into account the statistical distribution of crystal orientation in our case, it will always exist crystals whose more favourable orientations ( $\vec{d}_{v\max}$  near the normal of the substrate) will allow the virtual emergence to be eliminated. Thus, the fig.1E shows this elimination of the virtual emergences previously illustrated in the fig.1D. Taking into account the unfavourable orientation of the virtual emergences that are created during the last step fig.1E (very weak angle between  $\vec{d}_{v\max}$  and the substrate), their will be rapidly eliminated by the selection rule. Therefore, we consider that the virtual emergences do not strongly affect the topography of diamond films. The virtual emergences disturb the topography all the less so since the film thickness increases. Therefore, the use of this model will be more difficult in the case of thin diamond films.

## Principles of the topography determination

With the family of apices obtained by the homothetic growth of crystals, the software calculates the family of doublets  $(x,z)$  that define segments of lines. These ones correspond to the intersection between the crystalline faces of crystals and the  $y_i$  plane normal to the reference axis  $y$ . Then, the software searches for the segment family that characterises the bidimensional section  $y_i$  and memorises their crystalline character. The topography is obtained by bidimensional section cumulating, and by using a sufficiently weak geometric pitch  $\Delta y$  to restore the three-dimensional details of the topography (fig.2). Taking into account that each crystal is defined from its centre by a triplet  $(x,y,z)$ , it should be noted that each bidimensional section only keeps information's proceeding from crystals located on both sides of the plan  $y_i$ . The interaction distance  $d_{inter}$  which separates this plan and the farthest crystal able to interact with  $y_i$ , is evaluated by the relationship :  $d_{inter} = \left| \vec{d}_{v\max} \right|$  where the  $\vec{d}_{v\max}$  norm corresponds to the largest radius of a crystal.

The resulting topography is constituted by a succession of bidimensional sections including each of them a serie of segments, and separated to each other by the distance  $\Delta y$ . Each segment is defined on the one hand by two triplets  $(x_i^j, y_i, z_i^j)$  and  $(x_f^j, y_i, z_f^j)$  that fix the position of the  $j$ th segment in the space, and on the other hand by a data which identifies the nature of the  $\{hkl\}$  face and the crystal reference (among the  $p/100$  crystals located on the unit surface) that it corresponds. For example, we reported fig.3 four topographies that are calculated for different synthesis times, for a nucleation density  $\rho = 6 \times 10^3 \text{ mm}^{-2}$ , a growth rate  $V_{100} = 0.5 \text{ } \mu\text{m.h}^{-1}$ , a growth parameter  $\alpha = 1.8$  and a geometric pitch  $\Delta y = 0.05 \text{ } \mu\text{m}$ . These topographies corroborate the correct progress of the different calculus steps, and simulate the beginning of the coalescence step (arrows on the fig.3B). The figure 3 also reveals the presence of a virtual emergence (arrows on the fig.3C) that disappears for a higher synthesis time (fig.3D).

## Evolution of $R_{\{hkl\}}$ ratio during the growth of a polycrystalline coating

In order to illustrate the potentiality of this type of three-dimensional simulation, we have studied the evolution of the surface ratio  $R_{\{hkl\}} = \left( \frac{S_{\{100\}}}{S_{\{100\}} + S_{\{111\}}} \right)$  according to the synthesis time, for a growth with the following conditions :  $\rho = 10^5 \text{ mm}^{-2}$ ,  $V_{100} = 0.5 \text{ } \mu\text{m.h}^{-1}$ ,  $\alpha = 2$ , and  $\Delta y = 0.05 \text{ } \mu\text{m}$ . In a general case, the calculus of the total surface  $S_{\{hkl\}}$  for the complete topography ( $10^4 \text{ } \mu\text{m}^2$ ) that is constituted by  $(100/\Delta y)$  bidimensional sections and including  $n$  segments, can be evaluated by the relationship :

$$S_{\{hkl\}} = \sum_{y=0}^{100-\Delta y} \sum_{j=1}^N \sqrt{(x_f^j - x_i^j)^2 + (z_f^j - z_i^j)^2}$$

where the doublet  $(x_i^j, z_i^j)$  corresponds to the co-ordinates of the initial end of the  $\{hkl\}$  segment  $j$ , and  $(x_f^j, z_f^j)$  the co-ordinates of the final end of this segment. If  $\Delta y$  is weak enough, the algebraic  $\sum S_{\{hkl\}}$  of the calculated surfaces is representative of the topography.  $R_{\{hkl\}}$  that we can deduce and its evolution according to synthesis time allow us to validate the progressive formation of a film with a  $\{100\}\{111\}\langle 100 \rangle$  global morphology (fig.4). This morphology has been predicted in a previous paper [7] for a growth parameter equal to 2. The asymptotic evolution shown fig.4 suggests that from a given thickness, the evolutionary selection produces a stable global morphology with a  $R_{\{hkl\}}$  value that only depends on the growth parameter  $\alpha$ . the synthesis time necessary to obtain a continuous film is evaluated when the ratio  $S_{\text{substrate}}/S_{\text{diamond}}$  is negligible. Subsequent simulations carried out for higher nucleation density and various  $\alpha$  values should precise these results.

## Conclusions and perspectives

We have proposed a three-dimensional simulation of CVD diamond growth, that should allow us to access several physical and structural parameters associated to the surface of the film in the limit of the stated hypotheses (homothetic growth, absence of secondary nucleation and multiply twinned particles, negligible virtual emergences). In the field of materials, the previously defined  $R_{\{hkl\}}$  ratio is very attractive insofar as it gives a semi-quantitative information about the texture, and indicates the main crystalline facets exposed to the plasma (facets responsible of the subsequent diamond growth). This information is essential since the structural defects only appear in the volumes resulting to the growth of the  $\{111\}$  faces [14]. In order to precise the progressive formation of the texture, it is possible to reconstitute x-ray pole figures during the film growth, and to draw its evolution according to the thickness or  $\alpha$ . These figures, associated with the  $R_{\{hkl\}}$  ratio allow us to more precisely define the global morphology  $\langle hkl \rangle \{h_1 k_1 l_1\} \{h_2 k_2 l_2\}$  for a given film. For each topography, the knowledge of the grain boundary position can permit the calculus of the grain boundary density for a given thickness, and we can consequently determine a distribution map of volume defects linked to the coalescence between the crystals. Concerning the surface mechanics, the classical parameters of roughness ( $R_a$ ,  $S_k$ ,  $S_m$ ...) are calculable and can be studied in relation to

the growth conditions (nucleation density, growth parameter, growth rate). These tribological parameters, besides their interest in the functional mechanical applications, can be integrated in an in situ optical process control of CVD diamond growth previously described [15], where the roughness modifies the emissive behaviour of material.

In this paper, we have treated simple cases where  $\alpha$  is identical for each crystal, and the nuclei orientation is fixed in an aleatory manner. It is possible to affect specific parameters to each crystal that are different of neighbouring. Therefore, a more realistic simulation will consist to set these parameters according to a statistical distribution like a gaussian curve. The simulation of a heteroepitaxial film growth will be realised by a gaussian distribution of Euler angles that characterise the orientation of each nuclei. These different simulations are actually in preparation and will be soon correlated to the real diamond growth. The present model is mainly limited by the approximation concerning the neglected effect of the virtual emergences. A modification of this model is envisaged to correctly eliminate these emergences at the step of the bidimensional section calculus.

## References

- [1] A. Van der Drift, *Philips Res. Rep.*, 22 (1967) 267.
- [2] Y.J. Baik and K.Y. Eun, *Thin solid films*, 214 (1992) 123.
- [3] R.E. Clausing, L. Heatherly, L.L. Horton, E.D. Specht, G.M. Begun, Z.L. Wang  
*Diamond and Relat. Mater.*, 1 (1992) 411.
- [4] W. Müller-Sebert, C. Wild, P. Koidl, N. Herres, J. Wagner, T. Eckermann  
*Mat. Sci. Eng.*, B11 (1992) 173.
- [5] C. Wild, R. Kohl, W. Müller-Sebert, P. Koidl, *Diamond and Relat. Mater.*, 3 (1994) 373.
- [6] S. Barrat, I. Dieguez, H. Michel, E. Bauer-Grosse  
*Diamond and Relat. Mater.*, 3 (1994) 520.
- [7] S. Barrat, E. Bauer-Grosse, *Diamond and Relat. Mater.*, 4 (1995) 419.
- [8] C. Wild, N. Herres, P. Koidl, *J. Appl. phys.*, 68 (1990) 973.
- [9] C. Wild, P. Koidl, W. Müller-Sebert, H. Walcher, R. Kohl, N. Herres, R. Locher  
R. Samlenski, R. Brenn, *Diamond and Relat. Mater.*, 2 (1993) 158.
- [10] R. Hessmer, M. Schreck, B. Stritzker, *Diamond and Relat. Mater.*, 4 (1995) 416.
- [11] A.J. Dammers, S. Radelaar, *Materials Science Forum*, 94-96 (1992) 345.
- [12] J.M. Thijssen, H.J.F. Knops, A.J. Dammers, *Phys. Rev. B*, 45 (1992) 8650.
- [13] J.M. Thijssen, *Phys. Rev. B*, 51 (1995) 985.
- [14] N. Bozzolo, S. Barrat, I. Dieguez, E. Bauer-Grosse, *Acta. Met.* (submitted for publication).



- [15] S. Barrat, P. Pigeat, E. Bauer-Grosse, B. Weber, *Thin Solid Film*, 263 (1995) 127.

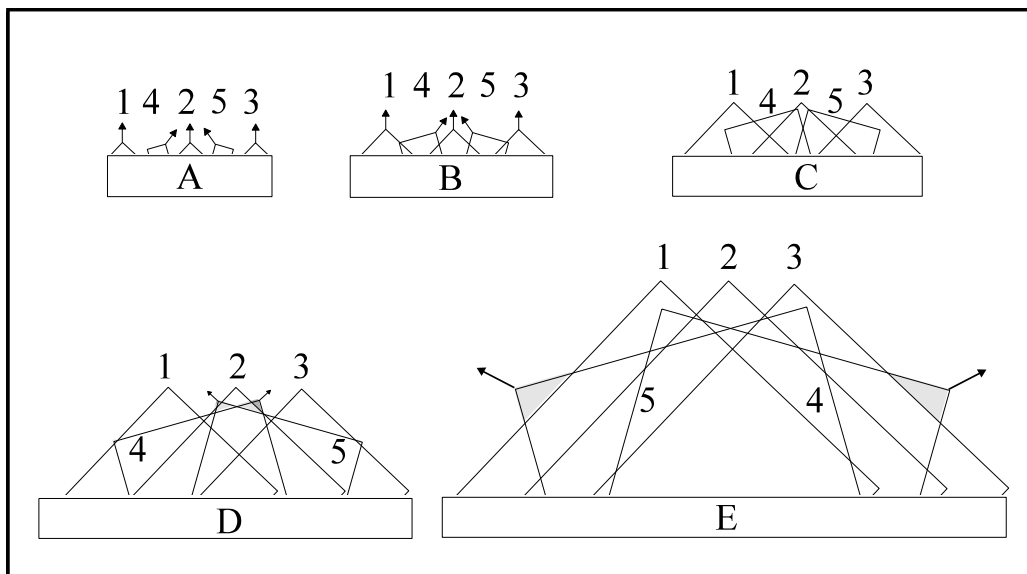


Figure 1

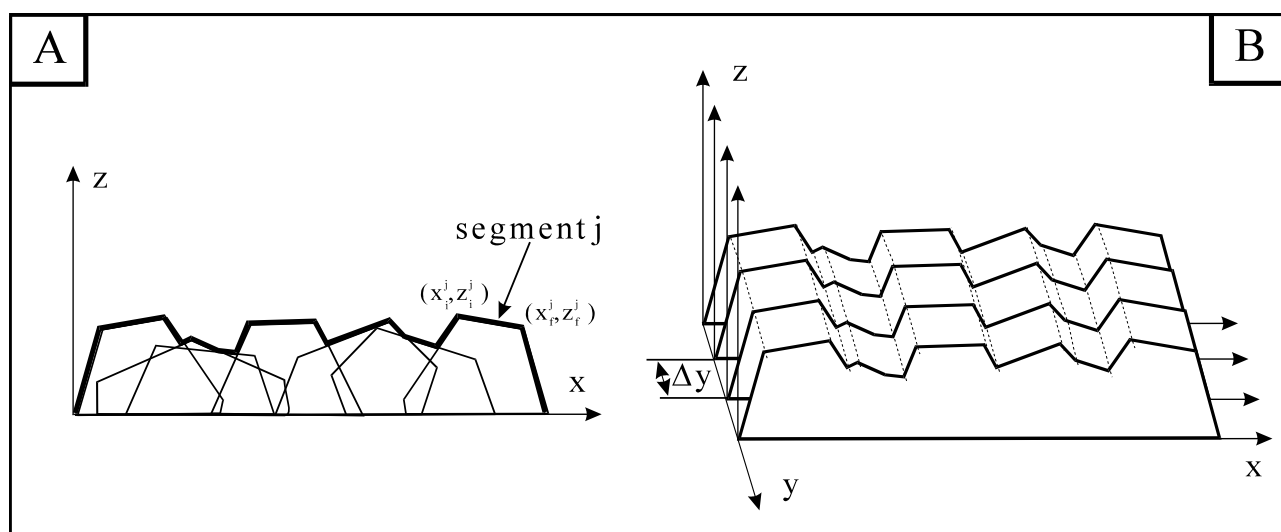


Figure 2

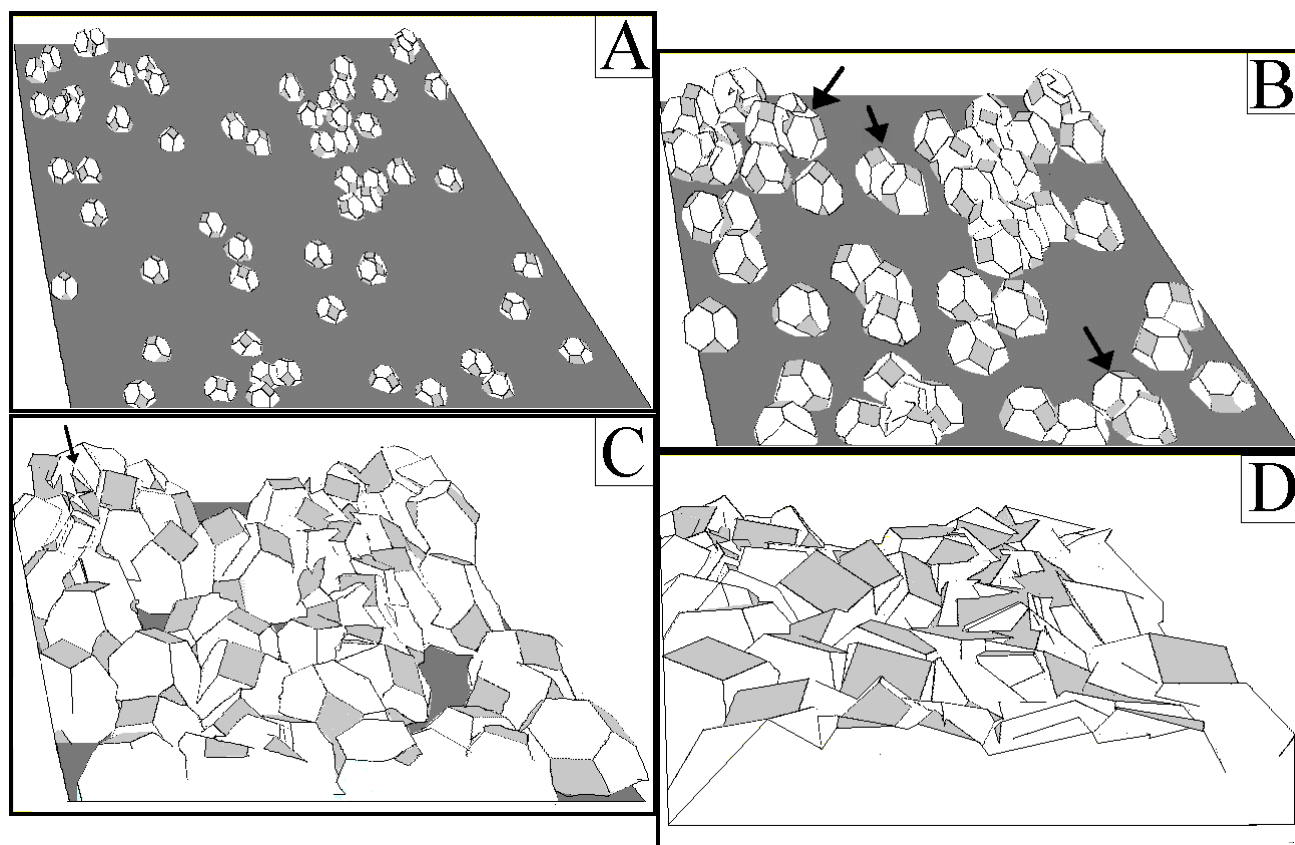


Figure 3

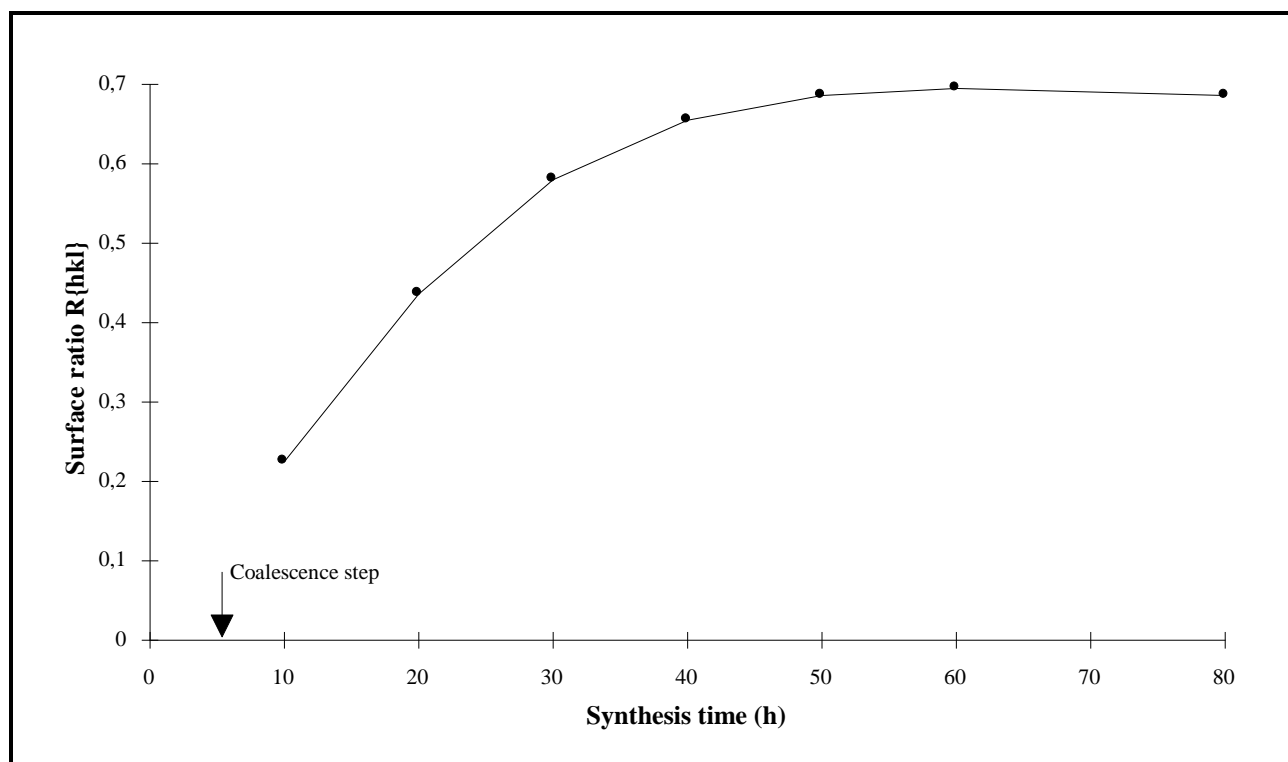


Figure 4

**Figure 1 :** bidimensional crystal growth.

A to C : growth with volume interpenetrations

D and E : growth with formation of virtual emergences (dashed areas)

**Figure 2 :** creation of a topography

A : calculus of a bidimensional envelope

B : cumulative effect of envelopes

**Figure 3 :** three-dimensional growth.  $\rho = 6 \times 10^3 \text{ mm}^{-2}$ ,  $V_{100} = 0.5 \text{ } \mu\text{m.h}^{-1}$ ,  $\alpha = 1.8$ , and  $\Delta y = 0.05 \text{ } \mu\text{m}$ .

$\{111\}$  faces : white areas,  $\{100\}$  faces : lightgray, substrate : darkgray.

Synthesis time (A) : 5 h, (B) : 10 h, (C) : 20 h and (D) : 40 h.

**Figure 4 :**  $R_{\{hkl\}}$  evolution according to the synthesis time for the following parameters :

$\rho = 10^5 \text{ mm}^{-2}$ ,  $V_{100} = 0.5 \text{ } \mu\text{m.h}^{-1}$ ,  $\alpha = 2$ , and  $\Delta y = 0.05 \text{ } \mu\text{m}$ .